Ind. J. Pharm. Edu. Res., 2026; 60(4s):s1657-s1668.
https://www.ijper.org

Original Article

Evaluation of the Anticancer Activity of Conessine against Human Melanoma (SK-MEL-28) Cells via Mitochondrial-Mediated Apoptotic Pathway

Yahya Hasan Hobani*

Department of Medical Laboratory Technology, College of Nursing and Health Sciences, Jazan University, Jazan, SAUDI ARABIA.

ABSTRACT

Background: Conessine is a steroidal alkaloid with diverse pharmacological activities, but its anticancer potential against melanoma and the mode of action remain poorly understood. **Objectives:** The present study evaluated the anticancer activity of conessine against human melanoma SK-MEL-28 cells and investigated its involvement in mitochondrial-mediated apoptosis. **Materials and Methods:** The cytotoxic effect of conessine was assessed using the MTT assay. Mitochondrial superoxide generation, membrane potential, induction of apoptosis, caspase-3 activity, and expression of apoptosis-related genes were examined using MitoSOX™ Red staining, flow cytometry, indirect ELISA, and real-time PCR, respectively. **Results:** Conessine significantly reduced SK-MEL-28 cell proliferation in a concentration-dependent manner (IC_{50}=76.78 µg/mL), whereas lower toxicity was observed in Human Dermal Fibroblast (HDF) cells (IC_{50}=143.33 µg/mL). Treatment with conessine enhanced the production of mitochondrial superoxide (76.78 µg/mL) and induced mitochondrial membrane depolarisation (54.50%). Conessine increased caspase-3 activity (1.7-fold increase), upregulated BAX expression, downregulated BCL2 expression, and enhanced the apoptotic cell populations (≥ 60%). **Conclusion:** These findings demonstrated that conessine exerts selective anticancer activity against SK-MEL-28 melanoma cells by inducing mitochondrial dysfunction and triggering the intrinsic apoptotic pathway. The study highlights conessine as a promising natural molecule for further development as a potential therapeutic agent against melanoma.

Keywords: Anti-apoptosis, BAX, BCL2, Caspase-3, Mitochondrial Apoptosis, Reactive Oxygen Species.

Correspondence:
Dr. Yahya Hasan Hobani
Department of Medical Laboratory Technology, College of Nursing and Health Sciences, Jazan University, Jazan, SAUDI ARABIA.
Email: yahobani@jazanu.edu.sa

Received: 21-05-2026;
Revised: 19-06-2026;
Accepted: 07-08-2026.

INTRODUCTION

Despite remarkable advancements in targeted therapies and immune checkpoint inhibitors, resistance to apoptosis continues to be a distinctive feature of melanoma tumor progression and treatment failure. Increasing data suggest that mitochondrial dysfunction and altered redox signaling play a crucial role in melanoma progression, metastasis, and resistance to chemotherapy. Therefore, treatment strategies aimed at restoring apoptotic sensitivity via mitochondrial targeting have emerged as a noteworthy thrust in current melanoma research. The incidence of melanoma is increasing globally, and the actual number of cases may be higher than the estimate in the registry.[1] Though several chemotherapeutic agents exhibit cytotoxicity and/or prolonged stabilisation of melanoma and other types of cancers, the improvement in survival rate is still questionable.[2] The attention towards natural medicine is increasing in the case of cancer treatment due to its wide range of availability, diverse structure, biological functions, and low toxicity.[3] Many natural products have been found to possess anti-cancer activity due to their involvement in autophagy, apoptosis, and regulation of various signalling pathways.[4]

Dysregulation of apoptotic pathways is a hallmark of cancer and contributes tumor progression and chemotherapy failure. Among the various apoptotic mechanisms, the intrinsic or mitochondrial-mediated pathway constitutes the main pathway in regulating cancer cell survival.[5] Numerous plant-derived compounds, especially alkaloids, have shown the ability to inhibit tumor growth through induction of oxidative stress, mitochondrial dysfunction, and apoptosis.[6] Conessine is a steroidal alkaloid, naturally present in the medicinal plant *Holarrhena antidysenterica* (L.), which has been widely used in traditional medicine to treat various diseases.[7] A few studies have investigated the anticancer potential of conessine in cancer cells; however, the research on melanoma cells is scarce. Specifically, the knowledge on the involvement of conessine in mitochondrial

DOI: 10.5530/ijper.20265707

oxidative stress and intrinsic apoptotic signaling is limited. With the goal of assessing conessine's anticancer efficacy against human melanoma SK-MEL-28 cells and to elucidate the underlying molecular mechanisms, the present investigation was designed. Conessine's cytotoxic effects on normal Human Dermal Fibroblast (HDF) cells as well as on the SK-MEL-28 cells were determined using the MTT assay and morphological observations. To ascertain the impact of conessine on the mitochondrial-mediated apoptotic pathway, additional research was conducted on mitochondrial superoxide generation, mitochondrial membrane potential disruption, apoptosis induction, caspase-3 activation, and expression of important apoptosis-related genes (BAX and BCL2). These findings may strengthen the existing evidence supporting the use of naturally derived molecules as potential therapeutic agents for melanoma treatment.

MATERIALS AND METHODS

Cell Line Culturing and Compound Preparation

This study utilises a human skin cancer cell line (SK-MEL-28) to investigate the anticancer potential of conessine, which was procured from ATCC, USA. Dulbecco's Modified Eagle's Medium (DMEM), bought from Sigma Aldrich (USA), was enriched by adding Fetal Bovine Serum (FBS), Sodium Bicarbonate ($NaHCO_3$), and L-glutamine. Antibiotics, including Streptomycin (100 µg/mL), Penicillin (100 U/mL), and Amphotericin B (2.5 µg/mL), purchased from Merck (Germany), were added to prevent microbial contamination. Incubation in a humidified CO_2 (5%) incubator (NBS Eppendorf, Germany) at 37°C enhances cell growth, the rate of which was evaluated by an inverted phase-contrast microscope (Olympus CKX41 with Optika Pro5 CCD camera) followed by the MTT (3-(4,5-dimethylthiazol-2-yl)-2,5-diphenyltetrazolium bromide) assay. After trypsinisation, the required number of wells was loaded with growth medium (10%) and SK-MEL-28 cell suspension (100 µL) in a 96-well tissue culture plate, consisting of a concentration of 5 × 10^3 cells/well, and incubated for 24 h before performing the experiments. Additionally, the Human Dermal Fibroblast (HDF) cells (HIMEDIA), cultured in Fibroblast Expansion medium, were supplemented with the aforementioned antibiotics to evaluate the cytotoxicity of conessine. A working solution of conessine was prepared using 0.1% Dimethyl Sulphoxide (DMSO) (1:1 ratio) and sterilised by a Millipore syringe filter (0.22 µM).

Qualitative and Quantitative Determination of Conessine's Anticancer Activity

Freshly prepared conessine solution at concentrations of 0, 6.25, 25, 50, and 100 µg/mL, was added to the SK-MEL-28 and HDF cell precipitates suspended in DMEM and incubated in a humidified CO_2 incubator overnight. Morphological characteristics of SK-MEL-28 and HDF cells were observed using an inverted phase contrast tissue culture microscope. For the MTT assay, 30 µL of reconstituted MTT solution (MTT + PBS) was added to the SK-MEL-28 cell culture ($5x10^3$ cells) and incubated for 4 hr. MTT solubilisation solution (Sigma-Aldrich, USA) was added to the cell precipitate to solubilise the formazan crystals and the absorbance was measured at a wavelength of 540 nm.[8] The percentage of viability was calculated by the formula:

$$\text{Percentage of Viability} = \frac{\text{Mean OD of sample}}{\text{Mean OD of control}} \times 100$$

The selectivity index of Conessine has been calculated using the formula:

$$\text{Selectivity Index (SI)} = \frac{IC_{50} \text{ in normal cells}}{IC_{50} \text{ in cancer cells}}$$

Determination of Mitochondrial Superoxide levels

Intracellular mitochondrial superoxide levels were determined as per the manufacturer's instructions found in the MitoSOX™ Red mitochondrial superoxide indicator with minor modifications. A stock solution of MitoSOX™ Red (5 mM) was prepared by dissolving in anhydrous DMSO. Working concentrations ranging from 1 µM to 100 nM were prepared from the stock by diluting in Hank's Balanced Salt Solution (HBSS) supplemented with calcium and magnesium, to achieve optimal signal-to-noise ratio with minimum cytotoxicity. SK-MEL-28 cells (2×10^4 cells/well) with approximately 60-70% confluency were treated with the IC_{50} of conessine and incubated overnight along with untreated control wells. An adequate volume of MitoSOX™ Red working solution was added to completely cover the cell precipitate and incubated for about 15 M in the dark. Excess dye was removed, and cells were resuspended in HBSS phenol-red-free medium prior to analysis.[9] Optimal excitation/emission was read at 510/580 nm using an inverted microscope equipped with a green fluorescence filter set. Fluorescence levels have been measured using a Qubit 2 Fluorometer, and Relative Fluorescence Units (RFU) have been measured.

Determination of Apoptosis

SK-MEL-28 cells (5×10^3 cells) treated with conessine (IC_{50}) were incubated for 24 hr and transferred to 12×75-mm polystyrene tubes.[10] The cell pellet was collected by centrifugation at 3000 rpm for 5 M and mixed with Muse™ Annexin V & Dead Cell Reagent (100 µL) and vortexed for 20 M at room temperature in a dark environment. Flow cytometer measurements were gated against untreated control cells and analysed for apoptosis using Muse FCS 3.0 software.

Determination of Mitochondrial Membrane Potential

Conessine-treated (IC_{50}) SK-MEL-28 cells were trypsinised and subjected to flow cytometry as per the following procedures.[11] The cells were resuspended in 95 µL of working solution of Muse™ MitoPotential dye (1:1000 ratio of dye and 1X assay buffer), and the mixture was incubated for 20 M. Prior to loading the sample to the flow cytometer (Millipore, USA), 5 µL of Muse MitoPotential

7-AAD was added to each well and mixed by vortexing, followed by incubation for 5 M.

Caspase 3 determination by ELISA Test

After incubating the conessine-treated SK-MEL-28 for 24 hr, the supernatant was maintained at 37°C overnight in a 96-well plate. 200 µL of blocking buffer (0.2% gelatin in 0.05% Tween 20: Merck; Germany) was added to the well-drained and PBS-washed wells. At room temperature, every 2 hr interval, primary antibody Caspase 3 (Santacruz), followed by PBS-TWEEN, secondary antibody (100 µL) (HRP Conjugate, Santacruz, USA) was added. After 1 hr, O-dianizidine hydrochloride (1 mg/100 mL methanol + 21 mL citrate buffer pH 5 + 60 mL H_2O_2: Sigma-Aldrich, USA) was added to the washed wells, followed by a 30 M incubation; 5 N HCl was added to stop the reaction.[12] Absorbance was read at 415 nm, and the activity of caspase 3 was calculated by dividing the OD Value by the standard protein concentration.

Determination of gene expression in conessine-treated melanoma cells

Total RNA has been isolated from conessine-treated SK-MEL-28 cells by TRIzol method as instructed by the manufacturer (Invitrogen- Product code 10296010). The addition of TRIzol solution (1 mL) and 5 M incubation causes the release of RNA. The addition of chloroform (200 µL) following centrifugation at 14000 rpm for 15 M (4°C), accumulates nuclear material in the aqueous phase. Upon mixing with 100% isopropanol, RNA precipitates as a white pellet on the sides and bottom of the tube, which is then washed with 75% ethanol. RNA, obtained as pellets, was centrifuged, later dried and suspended in TE buffer (13).[13] Template complementary DNA (cDNA) was synthesised using the iScript cDNA Synthesis kit (Biorad, Cat# 1708891 master premix for first-strand cDNA synthesis). 20 µL of reaction mixture in an RNase-free tube consisting of 5x iScript reaction mix (4 µL), iScript Reverse (1 µL), RNA template (0.5 µg of total RNA), and sterile distilled water. The thermal cycler (Eppendorf Master Cycler) was programmed to perform cDNA synthesis and the cycling conditions as follows: priming at 25°C for 5 M, synthesis at 46°C for 20 M, and RT inactivation for 1 M at 95°C. Real-Time qRT-PCR analysis was performed in Lightcycler 96 (Roche) using SYBR Green Master Mix (G BIOSCIENCES, Product code-786-5062). The data obtained from the triplicates were analysed using the ΔΔCt method (using Light Cycler 96 SW 1.1 Software). After initial activation at 95°C for 2 M, 40 cycles of denaturation (10 s at 95°C), annealing (1 M at 58°C), and extension (1 min/kb at 72°C) were executed.[14] The primer details are provided in Table 1.

Statistical analysis

Data were obtained from three independent experiments and analyzed using GraphPad Prism software (version 6.0). Statistical comparisons among groups were performed using One-Way Analysis of Variance (ANOVA), followed by Duncan's multiple-range *post hoc* test. Differences were considered statistically significant at $p<0.05$ compared with the control group. The levels of statistical significance are indicated as $p<0.05$, $^{*}p<0.01$, and $^{**}p<0.001$.

RESULTS

Conessine Reduces the Viability of SK-MEL-28

The cytotoxic effect of conessine against human melanoma SK-MEL-28 cells was evaluated following 24 hr of treatment at varying concentrations. Microscopic images (Figures 1A-1F) demonstrated distinct morphological variations between the conessine-treated and untreated (control) cells. Untreated cells possess spindle-shaped morphology with intact cellular architecture and firm attachment (Figure 1A). Conessine exerted dose-dependent toxicity on SK-MEL-28 cells as the morphological damage was increased from lower to higher concentrations. 100 µg/mL of conessine exhibited extensive damage, including cell rounding, shrinking, loss of adherence and loss of integrity, suggesting pronounced cytotoxicity. In addition to the morphological damage, the MTT assay revealed a dose-dependent viability loss of SK-MEL-28 cells while treated with conessine (Figure 1G). Conessine treatment reduced viability to approximately 95, 76, 68, 57, and 44% at 6.25, 12.5, 25, 50, and 100 µg/mL, respectively. Statistical analysis indicated a significant reduction ($^{***}p<0.001$) in cell viability compared with the untreated cells. The IC_{50} value of conessine was found to be 76.78 µg/mL, as determined using ED_{50} PLUS V1.0 software, indicating moderate yet notable cytotoxic activity against melanoma cells. Hence, the selectivity index of conessine has been calculated and found to be 1.86

Effect of Conessine on the Viability of HDF Cells

The cytotoxic effect of conessine on normal HDF cells was assessed and the results indicated that treatment with lower concentrations (6.25 and 12.5 µg/mL) of conessine caused minor or negligible morphological changes, with cells predominantly maintaining their typical fibroblastic morphology (Figures

Table 1: The details of the primers used in Real-time quantitative reverse transcription PCR (qRT-PCR).

Oligo Name	Forward		Reverse	
	Sequence (5′->3′)	Tm	SEQUENCE (5′->3′)	Tm
BCL2	CCTGTGGATGACTGAGTA	53.7	GAGACAGCCAGGAGAAATCA	57.3
BAX	ACCAAGCTGAGCGAGTGTC	62.1	TGTCCAGCCCATGATGGTTC	59.4

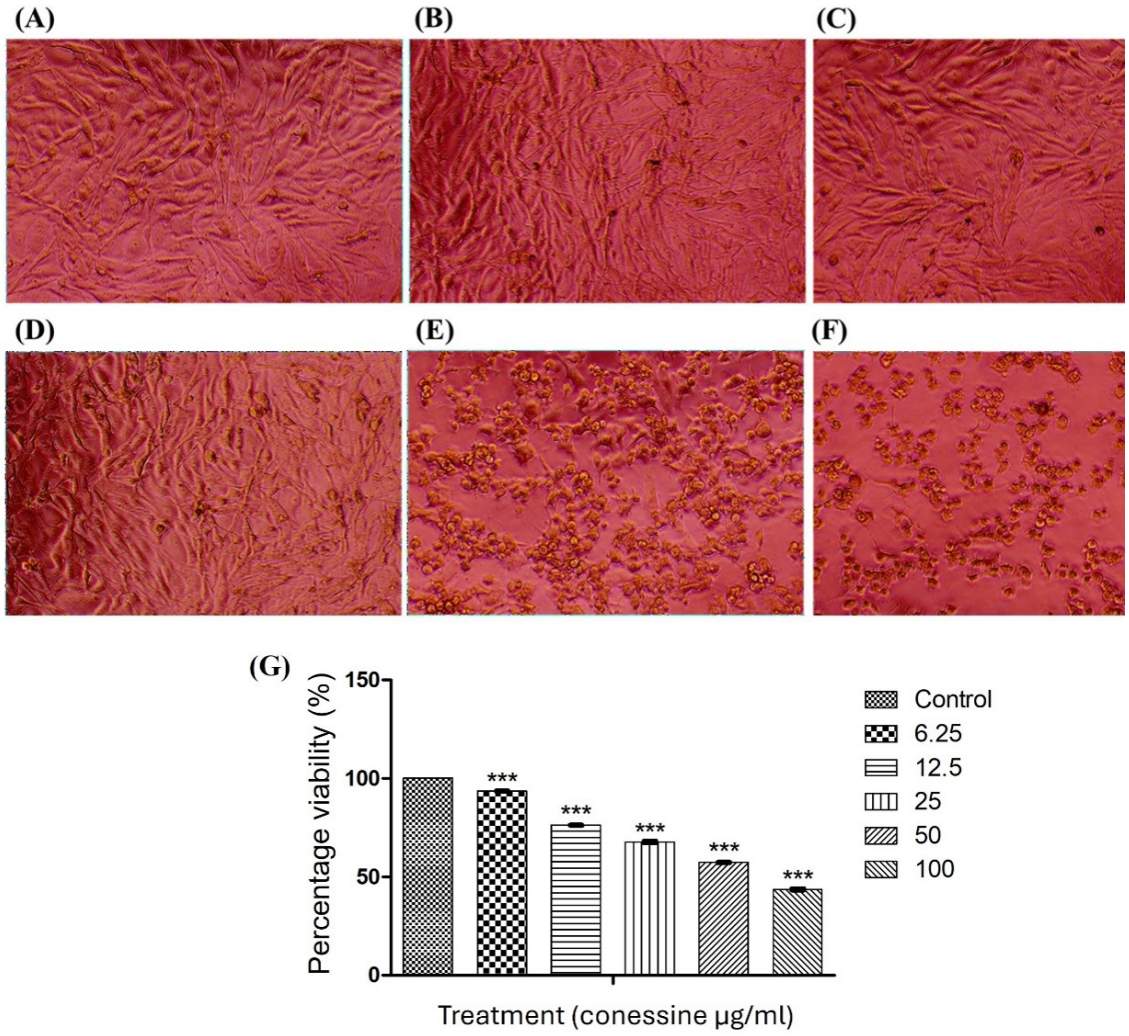

Figure 1: Effect of conessine on human melanoma SK-MEL-28 cell morphology and viability. A-F: Phase-contrast microscopic images demonstrating the morphological alterations induced by varying concentrations of conessine including 0 (untreated), 6.25, 12.5, 25, 50, and 100 µg/mL (starting from A to F). Control cells exhibited intact cellular architecture, whereas conessine-treated cells showed significant morphological alterations including cell shrinkage, rounding, loss of adherence, and reduced cell density. (G) MTT assay demonstrating the significant reduction of SK-MEL-28 cells' viability in a dose-dependent manner. Data are expressed as mean ± SD of triplicate experiments. Statistical significance was determined relative to the control group (***p<0.001).

2B-2C). Minor modifications in cellular architecture and slight decrease in cell density were observed at 25 and 50 µg/mL of conessine concentrations (Figures 2D, 2E). During treatment with a 100 µg/mL dose, partial cell shrinkage, mild detachment, and diminished confluency were observed, but the overall cellular architecture remained relatively intact (Figure 2F). MTT assay showed low cytotoxicity of conessine toward HDF cells. The viability of HDF cells was not affected, and it was comparable to that of untreated cells (Figure 2A) when 6.25 µg/mL conessine was used. The viability was gradually decreasing with the increased doses of conessine, attaining approximately 92, 86, 78, and 63% at 12.5, 25, 50, and 100 µg/mL, respectively (Figure 2G). Marked decreases in viability were noted at concentrations ≥12.5 µg/mL in comparison to the untreated control group (***p<0.001). The IC_{50} value of conessine against HDF cells was calculated as 143.336 µg/mL, indicating reduced cytotoxicity against normal fibroblast cells in comparison to SK-MEL-28 cells.

Conessine Induces Mitochondrial Superoxide (ROS) Generation in SK-MEL-28 Cells

Significant increase in MitoSOX™ Red fluorescence intensity was observed in SK-MEL-28 cells following 24 hr treatment with conessine (76.78 µg/mL). The weak basal red fluorescence in untreated cells indicates relatively low levels of ROS generation (Figure 3A). Conversely, conessine-treated SK-MEL-28 cells showed intense red fluorescence with increased intracellular signal accumulation, signifying enhanced mitochondrial oxidative stress and elevated superoxide production (Figure 3B). These observations were confirmed by the results of fluorometric analysis, which showed relative fluorescence intensity of roughly 1,300 RFU for the untreated group and 2,600 RFU for the conessine-treated groups. A two-fold rise in ROS level in treated groups demonstrated significant enhancement in fluorescence intensity (**p<0.01) (Figure 3C).

Conessine Induces Apoptosis in SK-MEL-28 Cells

Flow cytometric analysis demonstrated that conessine altered the apoptotic profile of SK-MEL-28 cells (Figures 4A, 4B). Conessine treatment significantly decreased viability to 36%, whereas it was 92.30% in the untreated control group. Due to conessine treatment, the apoptotic population increased from roughly 9% (in untreated cells) to over 60%, indicating a potential induction of programmed cell death. The quantitative analysis confirmed that conessine administration significantly reduced viability and dramatically increased apoptosis in comparison with the untreated controls (**p<0.01) (Figure 4C).

Conessine Induces Mitochondrial Membrane Depolarisation

The mitochondrial membrane potential was maintained in the untreated SK-MEL-28 cells, where among the viable cells, approximately 70.65% are polarised, 25.70% are depolarised, 1.55% are depolarised dead cells, and 2.10% are dead cells. Conversely, conessine-treated SK-MEL-28 cells exhibited a significant decrease in mitochondrial membrane potential, demonstrating a decreased proportion of viable polarised cells (54.50%) and an increased rate of live depolarised cells (42.30%). The rates of depolarised dead cells were 42.30% and 1.95%, respectively (Figures 5A and 5B). Conessine treatment significantly increased the rate of depolarised cells from 25% to nearly 40% post-treatment (**p<0.01) (Figure 5C).

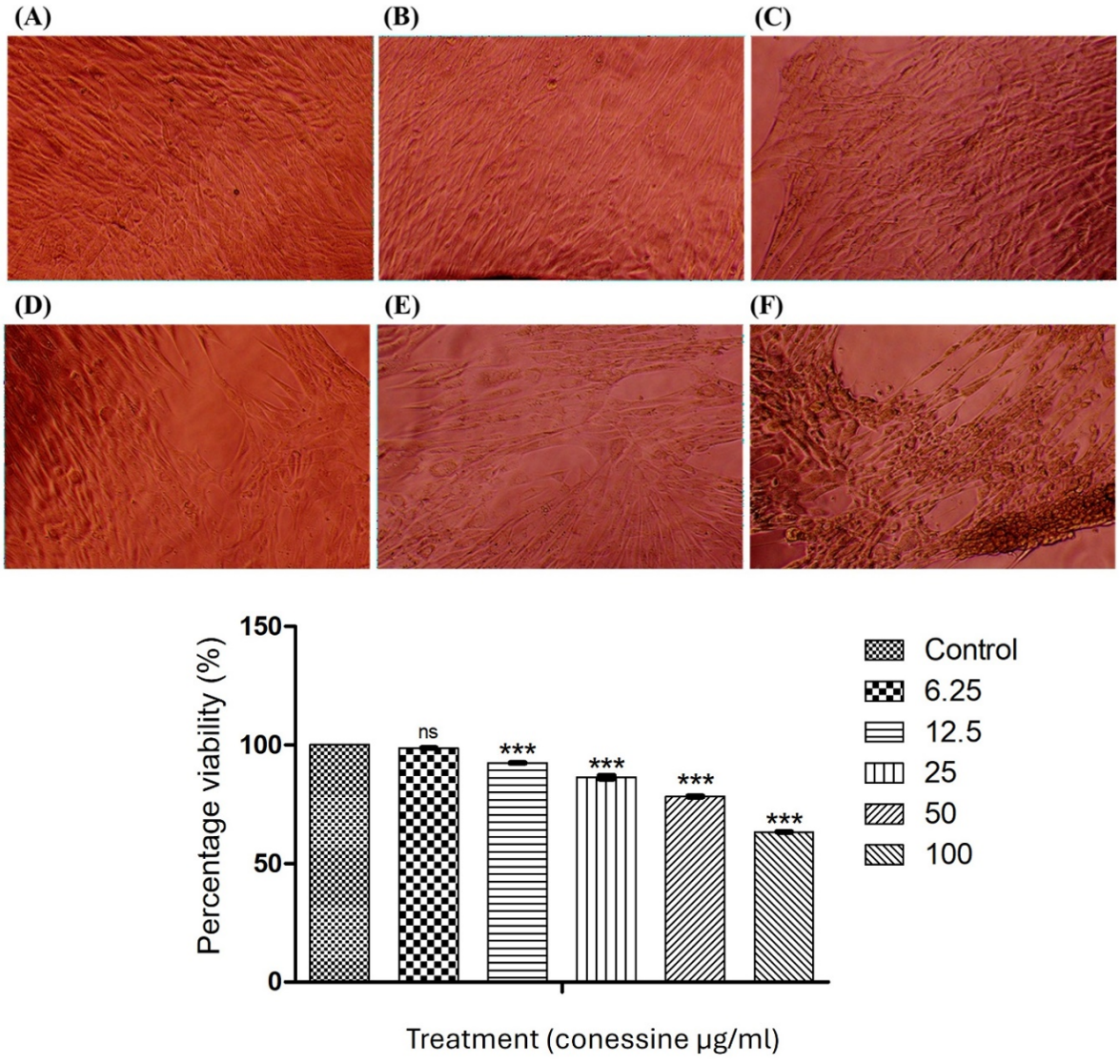

Figure 2: Effect of conessine on Human Dermal Fibroblast (HDF) cells morphology and viability. A-F: Phase-contrast microscopic images demonstrating morphological alterations induced due to 24 hr of varying concentrations of conessine including 0 (untreated), 6.25, 12.5, 25, 50, and 100 µg/mL (starting from A to F). Untreated HDF cells displayed intact cellular structure and adherence, whereas conessine-treated cells exhibited dose-dependent morphological alterations, including mild cell shrinkage, reduced confluency, and partial detachment at higher concentrations; (G) MTT assay showed a gradual dose-dependent reduction in HDF cell viability. Statistical significance was analysed relative to the control group (ns, non-significant; ***p<0.001).

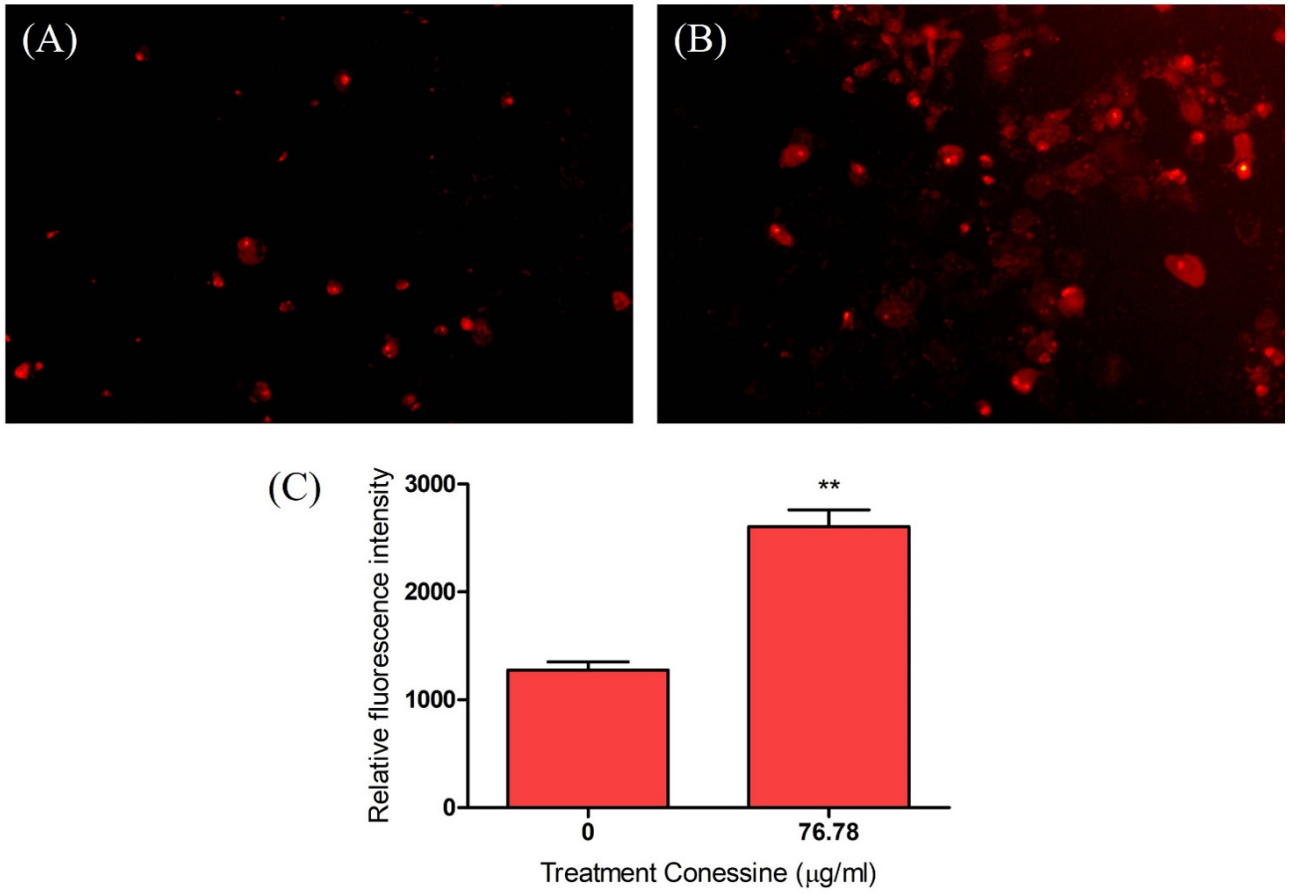

Figure 3: Qualitative and quantitative determination of conessine on mitochondrial superoxide generation in SK-MEL-28 cells. (A) - untreated control; (B) - conessine-treated (IC_{50}). (C) - Relative fluorescence intensity (RFU) measurement demonstrating a significant increase ($p<0.01$) in mitochondrial superoxide generation following conessine treatment, indicating increased mitochondrial oxidative stress.

Conessine Enhances Caspase-3 Activity

The indirect ELISA analysis revealed that the IC_{50} concentration (76.78 µg/mL) of conessine led to a notable elevation in caspase-3 activity in SK-MEL-28 cells relative to untreated controls (Figure 6). The baseline caspase-3 activity in untreated cells was around 0.7 activity units/mg protein, whereas treatment with conessine increased the activity to roughly 1.2 activity units/mg protein, reflecting a significant (*$p<0.05$) elevation of approximately 1.7-fold. The observed rise in caspase-3 activity implies the initiation of the execution phase of apoptosis in SK-MEL-28 cells after conessine exposure.

Conessine Modulates Apoptosis-Related Gene Expression

The qRT-PCR results demonstrated a marked alteration in apoptosis-related gene (BAX and BCL2) expression following conessine treatment. Conessine exposure upregulated the expression levels of the BAX gene to approximately 1.6-fold compared to untreated cells (Figure 7A). In contrast, conessine treatment downregulated BCL2 expression, with normalised basal expression levels (Figure 7B). The results of qRT-PCR revealed the reciprocal regulation of BAX and BCL2 following conessine treatment, and this effect indicates a shift in the intracellular apoptotic balance toward cell death.

DISCUSSION

Natural products can induce apoptosis in melanoma cells through various signaling pathways, including mediating endoplasmic reticulum stress, Wnt/β-Catenin, phosphoinositol-3-kinase/protein kinase B/mammalian target protein of rapamycin (pl3k/akt/mTOR), MAPK, and others.[4] An increasing number of studies have reported the anticancer activity of natural products, specifically targeting apoptosis-inducing mechanisms with low toxicity to normal cells.[4] The study on the antiproliferative potential of conessine in SK-MEL-28 human melanoma cells is currently scarce, making this study novel and providing insight into apoptosis-induced mechanisms associated with mitochondrial dysfunction and oxidative stress. The present study investigated the activation of the intrinsic mitochondrial apoptotic pathway by conessine (a plant product) via its effect on mitochondrial superoxide production, membrane depolarisation, and apoptotic induction, collectively suggesting its anticancer activity.

Initially, the result obtained from the MTT assay showed significant, concentration-dependent inhibition of SK-MEL-28 cell viability following 24 hr exposure. Morphological alterations, including cell rounding, shrinking, loss of adhesion and density, further confirm the cytotoxicity of conessine. IC_{50} value of 76.78 µg/mL exhibits effective suppression of cellular proliferation, indicating the cytotoxic potential of conessine against melanoma cells. Morphological alterations, including cell shrinkage and blebbing of the plasma membrane, are indicative of apoptosis, which is additionally associated with characteristic changes in nuclear morphology.[15] Pinzaru *et al.* calculated the IC_{50} value of 47.44 ± 2.41 µM for Rutin (a natural compound) in SK-MEL-28 cells.[16] Similarly, curcumin decreases cell viability in the MTT assay, and the IC_{50} was measured as 40 µM, and the morphological changes characteristic of apoptotic cell death were detected.[17] In the present study, the observed IC_{50} value of 76.78 µg/mL for conessine against melanoma cells indicates moderate yet biologically meaningful cytotoxic activity. The cytotoxic activity of natural products, particularly involving alkaloids and phytochemicals, is not interpreted solely based on cytotoxicity studies, but also on other mechanistic evidence.[18] The accompanying apoptotic and mitochondrial alterations observed in this study support the biological significance of conessine against melanoma cells. Moreover, the cytotoxic effect of conessine against HDF cells was 143.336 µg/mL, indicating reduced cytotoxicity against normal fibroblast cells compared to SK-MEL-28 cells. The above observations highlight a level of selective toxicity of conessine towards melanoma cells, despite

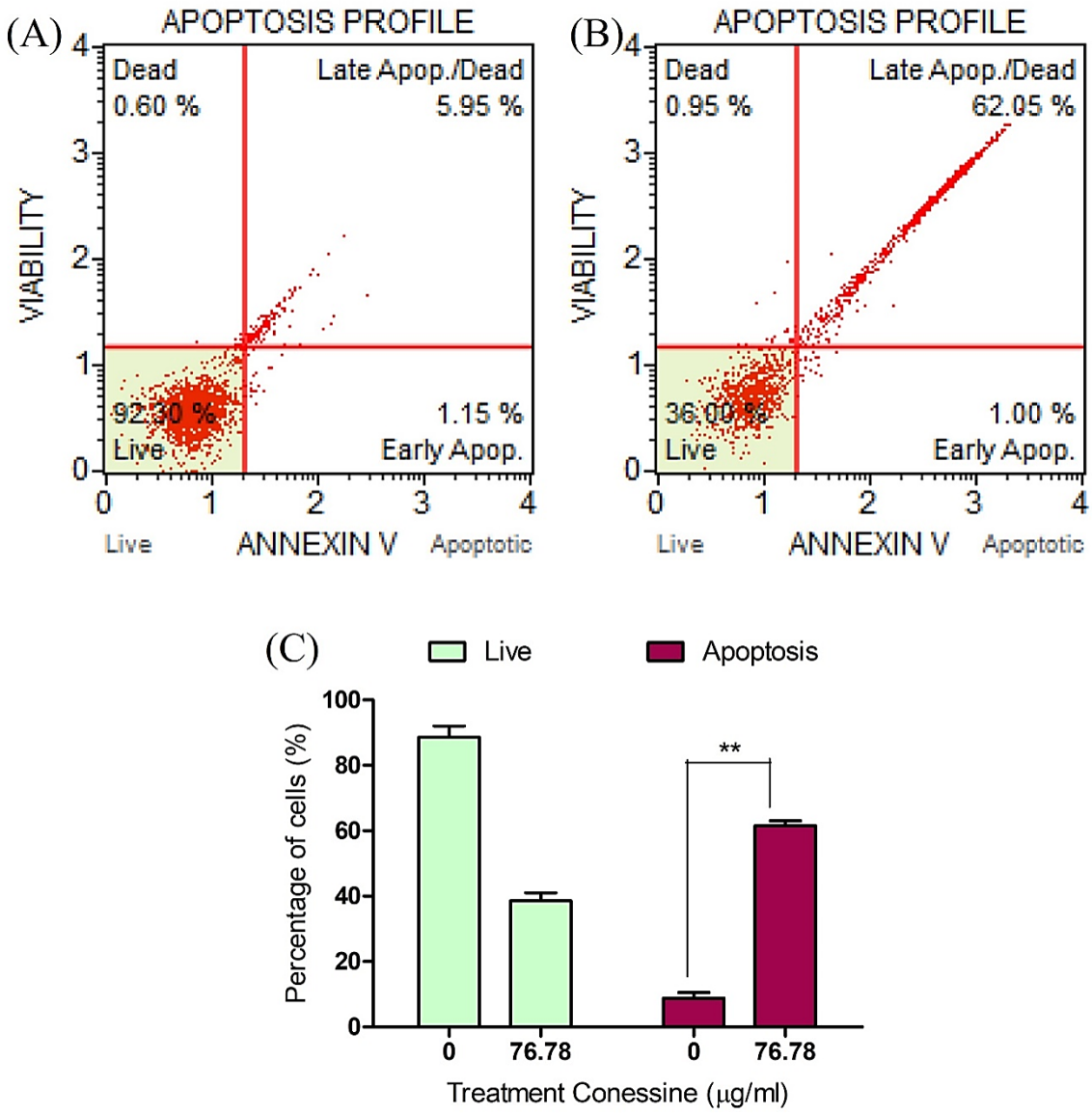

Figure 4: Annexin V apoptosis profile showing efficacy of conessine in inducing apoptosis in SK-MEL-28 melanoma cells. (A) - Untreated SK-MEL-28 cells showing a predominance of viable cells with minimal apoptotic and dead cell populations; (B) - Treatment of conessine (IC_{50}) demonstrating a marked increase in apoptotic cells and significant reduction in viable cells; (C) - Quantitative analysis showing significant ($p<0.01$) decrease in the percentage of viable cells and increased proportion of apoptotic cells compared with untreated controls.

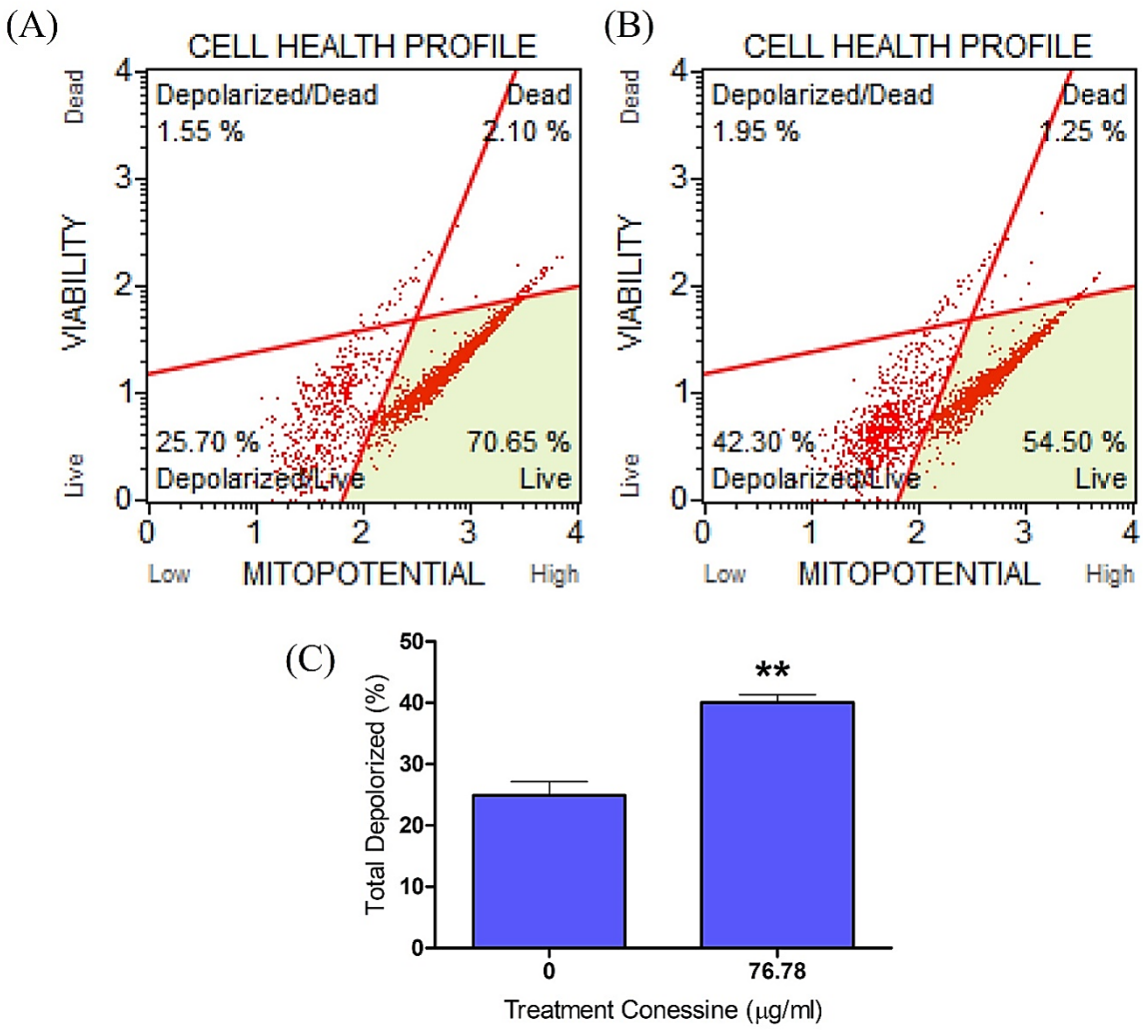

Figure 5: Flow cytometric profile showing the effect of conessine on mitochondrial membrane potential in SK-MEL-28 cells. (A)- Untreated control group with predominant viable cells with mitochondrial membrane potential and a smaller proportion of cells exhibited mitochondrial depolarization; (B)- Conessine (IC_{50}) treatment markedly increased the population of cells with depolarized mitochondrial membranes and reduced the percentage of viable cells with intact mitochondrial membrane potential; (C) - Quantitative analysis indicated significant ($p<0.01$) increase in mitochondrial membrane depolarization due to conessine treatment compared with untreated control cells.

maintaining higher vitality in normal dermal fibroblasts. The inherent metabolic differences between malignant and healthy cells may underlie this selective reaction. Melanoma cells are frequently more susceptible to agents that impair mitochondrial function and increase intracellular Reactive Oxygen Species (ROS) levels above the thresholds.[19]

A major mechanistic finding of this study was the considerable increase in mitochondrial superoxide generation after conessine treatment, as shown by MitoSOXTM Red staining and fluorometric analysis. Mitochondria represent the primary intracellular source of ROS, which contributes to normal signaling and metabolic regulation, but excessive accumulation causes oxidative damage and initiates apoptotic signaling cascades.[20] Emerging melanoma research increasingly recognises that excessive generation of ROS weakens antioxidant defences, causes persistent mitochondrial damage, and eventually triggers cell death, whereas moderate ROS levels may promote tumor growth and proliferation.[21] A comparable rise in mitochondrial ROS has been reported by Lee *et al.* where a natural compound, Lucknolide A -10-undecenoyl (LA-UC), induced ROS in melanoma cells and increased MitoSOX fluorescence, indicating apoptosis, DNA damage, and mitochondrial dysfunction.[22] The ROS build-up may also explain the morphological alterations observed in the MTT assay. Excessive mitochondrial superoxide can disrupt the integrity of the mitochondrial membrane, which restricts ATP generation and respiration via oxidation reactions.[23] Such oxidative damage may cause cellular shrinkage, membrane blebbing, and decreased proliferative capacity, all of which were detected in conessine-treated SK-MEL-28 cells. Hence, the approximate two-fold increase (1300 to 2600 RFU) in mitochondrial superoxide observed in cells treated with conessine

indicates that oxidative stress is a key factor in mediating its cytotoxic effect.

Mitochondrial Membrane Potential (ΔΨm) analysis provided further insight into the association between ROS generation and mitochondrial integrity. In healthy mitochondria, a transmembrane electrochemical gradient regulates oxidative phosphorylation and ATP generation, the disruption of which leads to mitochondrial dysfunction and is an early indicator of intrinsic apoptosis.[23] In this study, after conessine treatment, live cell depolarisation has been significantly increased by 42%, showing substantial impairment of mitochondrial function. Peng *et al*. used H_2DCF-DA and TMRM staining and flow cytometry to evaluate ROS generation and mitochondrial membrane potential in melanoma cells treated with an Extracellular Signal-Regulated Kinase (ERK) inhibitor and Myeloid Cell Leukemia-1 (Mcl-1) inhibitor, resulting in a higher rate of depolarised cells (up to 79%).[24] Our study observed that 40% of the population is depolarised, which is slightly lower than the findings of the above study, which applied a dual-drug synergistic strategy together with multiple melanoma lines and assays. The significant association between ROS generation and mitochondrial depolarisation observed in this work confirms that oxidative stress accompanies mitochondrial damage.

The disruption of outer mitochondrial membrane integrity and opening of membrane transition pores facilitate the release of pro-apoptotic proteins into the cytosol and initiate downstream apoptotic signalling.[25] Flow cytometric Annexin V analysis demonstrated that conessine exposure resulted in a significant reduction of viable cell populations, along with a considerable rise in apoptotic cells. Annexin V binds to phosphatidylserine residues externalised during apoptosis, suggesting that conessine-induced cytotoxicity primarily occurs through programmed cell death. In the present study, the overall apoptotic population has increased from approximately 9% in control cells to at least 60% after conessine treatment. Apoptosis is usually characterised by increasing membrane permeability, chromatin condensation, and irreversible cellular decomposition subsequent to the activation of intracellular death signaling pathways.[5] A study by Sezer investigated the anticancer activity of escin in CHL-1 human melanoma cells using the same assay and observed a significant reduction in viable cells to approximately 62% in CHL-1 cells and an increase in total apoptosis, which is 37.72%.[26] In the present study, conessine treatment reduced viability to nearly 36% and increased the apoptotic population beyond 60% in SK-MEL-28 cells. The marked shift from viable to apoptotic populations supports the hypothesis that conessine-mediated cytotoxicity occurs through activation of apoptotic pathways, consistent with the observed mitochondrial oxidative stress and proposed mitochondrial-mediated apoptotic mechanism.

Further elucidation of the apoptotic mechanism induced by conessine, caspase-3 activity was determined using indirect ELISA. In the present investigation, conessine treatment significantly increased caspase-3 activity to 1.7-fold compared to untreated controls. In an earlier study, a ferruginol analogue increased the activity of caspase-3/7 to approximately 2.5-fold at 48 hr, in addition to exhibiting ROS increase, mitochondrial dysfunction, and apoptosis in SK-MEL-28 cells.[27] Caspases coordinate the proteolytic processes that lead to cellular disintegration, hence known as the main executioners of apoptotic cell death. In the present investigation, conessine treatment significantly increased caspase-3 activity to 1.7-fold compared to untreated controls. During intrinsic apoptosis, the release of cytochrome c and mitochondrial dysfunction precedes the activation of these caspases. Upon mitochondrial outer membrane permeabilisation, cytochrome c combines with Apoptotic protease activating factor-1 (Apaf-1) and procaspase-9 to synthesise the apoptosome, which later activates caspase-9 and caspase-3.[5] Therefore, the enhanced caspase-3 activity reported in our study supports the concept that conessine-induced apoptosis proceeds via mitochondrial-mediated signaling rather than nonspecific cytotoxic damage.

Further mechanistic evidence for intrinsic apoptosis was provided by qRT-PCR study on apoptosis-related genes.[28] Conessine treatment resulted in a shift in the BAX/BCL2 balance toward apoptosis. After treatment, the expression of the pro-apoptotic gene, BAX, was increased while the expression of the anti-apoptotic gene, BCL2, was decreased. BAX promotes apoptosis by facilitating membrane permeabilisation and the release of cytochrome c (apoptogenic proteins). On the other hand, BCL2 prevents pore formation and cytochrome c leakage, stabilising mitochondrial membranes and antagonising pro-apoptotic signals.[29] Comparable qRT-PCR results were obtained in a study by Zhang *et al*. where SK-MEL-28 melanoma cells treated

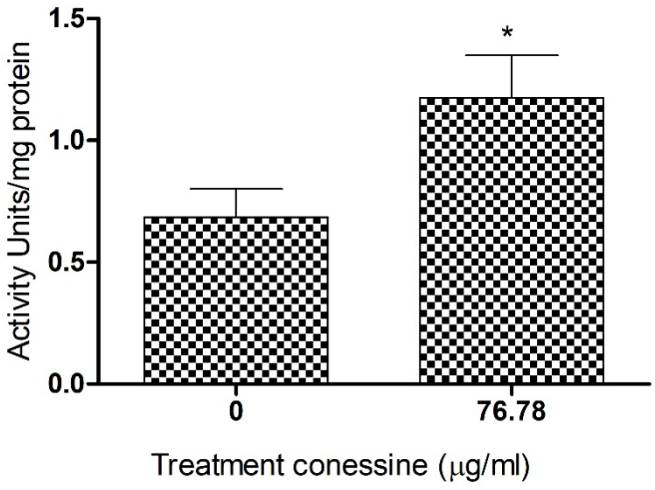

Figure 6: Determination of caspase-3 activity in SK-MEL-28 cells after conessine treatment (IC_{50}) for 24 h. Conessine significantly (*p<0.05) increased caspase-3 activity compared with untreated control cells, indicating induction of apoptotic signaling.

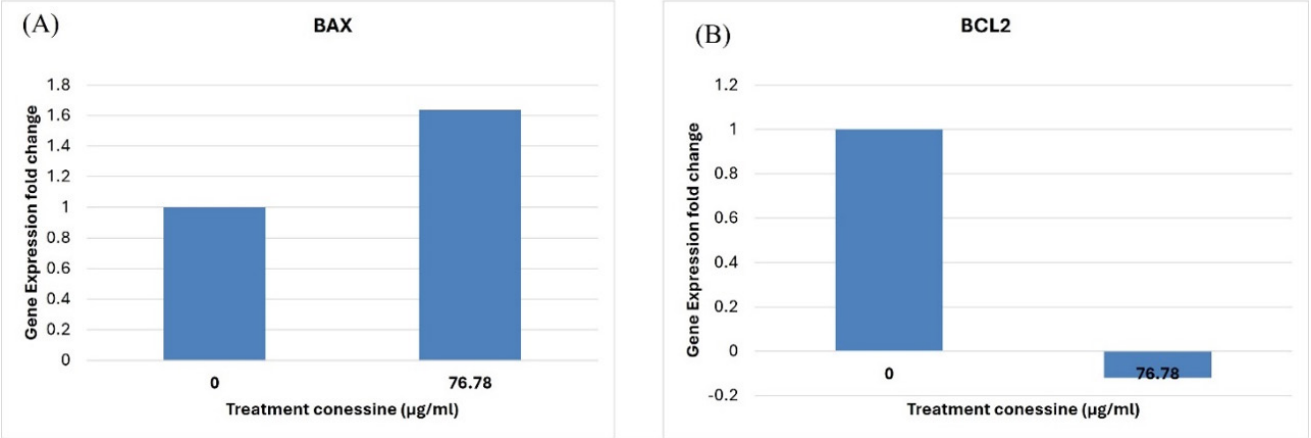

Figure 7: Quantitative real-time qRT-PCR results demonstrating the effect of conessine (IC_{50}) on the expression of apoptosis-related genes in SK-MEL-28 melanoma cells. (A) Upregulated mRNA expression of the pro-apoptotic gene, BAX; (B) Downregulated mRNA expression of the anti-apoptotic gene, BCL2.

with a Squalene-Derived Compound (SQ-diEG) demonstrated increased BAX expression and decreased anti-apoptotic BCL-xL gene expression.[30] Similarly, *Dendrobium Pearl Vera* extract demonstrated a shift in BAX/BCl-2 expression in SK-MEL-28 melanoma cells, proving the association of enhanced cytochrome-c and caspase expression with the activation of the intrinsic apoptotic pathway.[31] Therefore, the ratio of BAX to BCL2 is often considered to be a more effective indicator of apoptotic susceptibility.

CONCLUSION

On the whole, the current findings provide a rational order of mechanisms explaining conessine-mediated apoptosis in SK-MEL-28 melanoma cells. Initially, conessine treatment exerted the selective antiproliferative action by decreasing the viability of melanoma cells while maintaining less harm to normal dermal fibroblasts. The development of mitochondrial oxidative stress disrupts the integrity of the mitochondria, which leads to the collapse of ΔΨm and loss of the potential of the mitochondrial membrane. Increased apoptotic populations and caspase-3 activity cause mitochondrial failure. Finally, apoptotic commitment and mitochondrial permeabilisation are further boosted by the transcriptional regulation of BAX and BCL2. Mitochondrial-mediated apoptosis is becoming a largely acknowledged therapeutic target because melanoma cells possess dysregulated mitochondrial metabolism and altered redox signaling that make them susceptible to substances that induce oxidative stress. These results underscore conessine's potential as a viable natural medicinal possibility for the treatment of melanoma.

However, the present study has a few limitations that should be considered when interpreting the findings. First, no commercially available standard anticancer drug was included as a positive control; therefore, the anticancer efficacy of conessine could not be directly compared with that of an established therapeutic agent. Second, the mechanistic evidence for apoptosis was primarily based on mRNA expression and other functional assays, without protein-level validation by Western blot analysis of key apoptotic markers such as BAX, BCL-2, cleaved caspase-3, PARP, or cytochrome c. Third, the anticancer activity was evaluated using only a Single Melanoma Cell Line (SK-MEL-28), and therefore the findings cannot be generalized to other melanoma subtypes or cellular backgrounds. Validation using additional melanoma cell lines is warranted. Fourth, the study was limited to *in vitro* experiments, and the anticancer efficacy and safety of conessine have not yet been validated in appropriate *in vivo* models. Finally, the moderate IC_{50} value observed in the present study indicates that structural optimization of the conessine scaffold may be required to improve its potency and reduce the effective concentration. Future studies should therefore focus on structural modification and Structure-Activity Relationship (SAR) investigations, comparative evaluation with established anticancer drugs, validation of the proposed apoptotic mechanisms at the protein level, testing across multiple melanoma cell lines, and *in vivo* evaluation to further establish the therapeutic potential of conessine.

ABBREVIATIONS

SK-MEL-28: Human Melanoma Cell Line SK-MEL-28; **HDF:** Human Dermal Fibroblast; **MTT:** 3-(4,5-Dimethylthiazol-2-yl)-2,5-diphenyltetrazolium Bromide; **ELISA:** Enzyme-Linked Immunosorbent Assay; **PCR:** Polymerase Chain Reaction; **qRT-PCR:** Quantitative Real-Time Reverse Transcription Polymerase Chain Reaction; **IC_{50}:** Half Maximal Inhibitory Concentration; **BAX:** BCL2-Associated X Protein; **BCL2:** B-Cell Lymphoma 2; **ROS:** Reactive Oxygen Species; **ATCC:** American Type Culture Collection; **USA:** United States of America; **DMEM:** Dulbecco's Modified Eagle Medium; FBS**:** Fetal Bovine Serum; **$NaHCO_3$:** Sodium Bicarbonate; **CO_2:** Carbon Dioxide; **CCD:** Charge-Coupled Device; **DMSO:** Dimethyl Sulfoxide;

PBS: Phosphate Buffered Saline; **HBSS:** Hank's Balanced Salt Solution; **RFU:** Relative Fluorescence Unit; **FCS:** Flow Cytometry Standard; **7-AAD:** 7-Aminoactinomycin D; **HRP:** Horseradish Peroxidase; **H_2O_2:** Hydrogen Peroxide; **HCl:** Hydrochloric Acid; **OD:** Optical Density; **RNA:** Ribonucleic Acid; **TRIzol:** Tri Reagent Isolation Solution; **TE Buffer:** Tris-EDTA Buffer; **cDNA:** Complementary DNA; **RNase:** Ribonuclease; **SYBR:** SYBR Green Dye; **Ct:** Cycle Threshold; **ANOVA:** Analysis of Variance; **ED_{50}:** Median Effective Dose; **SD:** Standard Deviation; **ATP:** Adenosine Triphosphate; **ΔΨm:** Mitochondrial Membrane Potential; **ERK:** Extracellular Signal-Regulated Kinase; **Mcl-1:** Myeloid Cell Leukemia-1; **Apaf-1:** Apoptotic Protease Activating Factor-1; **BAK:** BCL2 Antagonist/Killer 1; **mRNA:** Messenger Ribonucleic Acid; **LA-UC:** Lucknolide A-10-Undecenoyl; **H2DCF-DA:** 2′,7′-Dichlorodihydrofluorescein Diacetate; **TMRM:** Tetramethylrhodamine Methyl Ester; **CCCP:** Carbonyl Cyanide m-Chlorophenyl Hydrazone; **FEBS:** Federation of European Biochemical Societies; **SQ-diEG:** Squalene-Derived Diethylene Glycol Compound; **Wnt:** Wingless/Integrated Signaling Pathway; **PI3K:** Phosphoinositide 3-Kinase; **Akt:** Protein Kinase B; **mTOR:** Mammalian Target of Rapamycin; **G2/M:** Gap 2/Mitosis Phase of the Cell Cycle.

CONFLICT OF INTEREST

The author declares that there is no conflict of interest.

SUMMARY

Conessine, a steroidal alkaloid derived from *Holarrhena antidysenterica*, was evaluated for its anticancer activity against human melanoma SK-MEL-28 cells. Conessine significantly reduced melanoma cell viability in a concentration-dependent manner, with an IC_{50} of 76.78 µg/mL, while exhibiting lower toxicity toward normal human dermal fibroblasts. Treatment increased mitochondrial superoxide generation, induced mitochondrial membrane depolarization, enhanced apoptosis, and elevated caspase-3 activity. Gene expression analysis revealed upregulation of the pro-apoptotic gene BAX and downregulation of the anti-apoptotic gene BCL2. These findings indicate that conessine exerts selective anticancer effects through mitochondrial-mediated apoptotic pathways, supporting its therapeutic potential against melanoma.

REFERENCES

1. Siegel RL, Giaquinto AN, Jemal A. Cancer statistics, 2024. CA Cancer J Clin. 2024;74(1):12-49. doi: 10.3322/caac.21820, PMID 38230766.
2. Algazi AP, Soon CW, Daud AI. Treatment of cutaneous melanoma: current approaches and future prospects. Cancer Manag Res. 2010;2:197-211. doi: 10.2147/CMR.S6073, PMID 21188111.
3. Wang M, Zhang Y, Ni S, Sun M, Wu Q, Wu X, *et al.* The anti-cancer activity of dioscin: an update and future perspective. Med Oncol. 2025;42(3):63. doi: 10.1007/s12032-024-02572-6, PMID 39899128.
4. Gao H, Huang J, Zhang D, Li S, Long S, Qin Y. Natural products as therapeutics for malignant melanoma: preclinical evidence and mechanism. Front Pharmacol. 2025;16:1641838. doi: 10.3389/fphar.2025.1641838, PMID 40932870.
5. Mustafa M, Ahmad R, Tantry IQ, Ahmad W, Siddiqui S, Alam M, *et al.* Apoptosis: a comprehensive overview of signaling pathways, morphological changes, and physiological significance and therapeutic implications. Cells. 2024;13(22):1838. doi: 10.3390/cells13221838, PMID 39594587.
6. Nelson VK, Nuli MV, Mastanaiah J, Saleem T S M, Birudala G, Jamous YF, *et al.* Reactive oxygen species mediated apoptotic death of colon cancer cells: therapeutic potential of plant derived alkaloids. Front Endocrinol. 2023;14:1201198. doi: 10.3389/fendo.2023.1201198, PMID 37560308.
7. Mustafa G, Musa SI, Shinde P, Eknure C, Bachhav Y, Paradkar A. Conessine, a steroidal alkaloid *from Holarrhena antidysenterica*: ethnomedical roots, pharmacological insights, and formulation strategies for modern drug development. Steroids. 2026;233-234:109799. doi: 10.1016/j.steroids.2026.109799, PMID 42134430.
8. Alhakamy NA, Ahmed OA, Fahmy UA, Md S. Development and *in vitro* evaluation of 2-methoxyestradiol loaded polymeric micelles for enhancing anticancer activities in prostate cancer. Polymers. 2021;13(6):884. doi: 10.3390/polym13060884, PMID 33805675.
9. Kalyanaraman B, Darley-Usmar V, Davies KJ, Dennery PA, Forman HJ, Grisham MB, *et al.* Measuring reactive oxygen and nitrogen species with fluorescent probes: challenges and limitations. Free Radic Biol Med. 2012;52(1):1-6. doi: 10.1016/j.freeradbiomed.2011.09.030, PMID 22027063.
10. Vermes I, Haanen C, Steffens-Nakken H, Reutelingsperger C. A novel assay for apoptosis flow cytometric detection of phosphatidylserine expression on early apoptotic cells using fluorescein labelled annexin V. J Immunol Methods. 1995;184(1):39-51. doi: 10.1016/0022-1759(95)00072-I, PMID 7622868.
11. Lee CM, Kang MA, Bae JS, Park K, Yang YH, Lee J, *et al.* An *in vitro* study on anti-carcinogenic effect of remdesivir in human ovarian cancer cells via generation of reactive oxygen species. Hum Exp Toxicol. 2022; 41. doi: 10.1177/09603271221089257.
12. Meyer P, Crowther JR. The ELISA guidebook. Methods Mol Biol. 2001; 149, Humana Press, Elsevier Masson.
13. Chomczynski P, Sacchi N. Single-step method of RNA isolation by acid guanidinium thiocyanate-phenol-chloroform extraction. Anal Biochem. 1987;162(1):156-9. doi: 10.1006/abio.1987.9999, PMID 2440339.
14. Livak KJ, Schmittgen TD. Analysis of relative gene expression data using real-time quantitative PCR and the 2ΔΔCT method. methods. Methods. 2001;25(4):402-8. doi: 10.1006/meth.2001.1262.
15. Kang S, Kim KR, Cho M, Hwang J, Yang JM, Kim JK, *et al.* High-resolution imaging of morphological changes associated with apoptosis and necrosis using single-cell full-field optical coherence tomography. Biosensors. 2025;15(8):522. doi: 10.3390/bios15080522, PMID 40862983.
16. Pinzaru I, Chioibas R, Marcovici I, Coricovac D, Susan R, Predut D, *et al.* Rutin exerts cytotoxic and senescence-inducing properties in human melanoma cells. Toxics. 2021;9(9):226. doi: 10.3390/toxics9090226, PMID 34564377.
17. Manica D, Silva GBd, Silva APd, Marafon F, Maciel SF, Bagatini MD *et al.* Curcumin promotes apoptosis of human melanoma cells by caspase 3. Cell Biochem Funct. 2023;41(8):1295-304. doi: 10.1002/cbf.3863, PMID 37792322.
18. Yusof WN, Abdullah H. Phytochemicals and cytotoxicity of *Quercus infectoria* ethyl acetate extracts on human cancer cells. Trop Life Sci Res. 2020;31(1):69-84. doi: 10.21315/tlsr2020.31.1.5, PMID 32963712.
19. An X, Yu W, Liu J, Tang D, Yang L, Chen X. Oxidative cell death in cancer: mechanisms and therapeutic opportunities. Cell Death Dis. 2024;15(8):556. doi: 10.1038/s41419-024-06939-5, PMID 39090114.
20. Chen S, Li Q, Shi H, Li F, Duan Y, Guo Q. New insights into the role of mitochondrial dynamics in oxidative stress-induced diseases. Biomed Pharmacother. 2024;178:117084. doi: 10.1016/j.biopha.2024.117084, PMID 39088967.
21. Ma N, Wang Y, Li X, Xu M, Tan D. Reactive oxygen species in cancer: mechanistic insights and therapeutic innovations. Cell Stress Chaperones. 2025;30(5):100108. doi: 10.1016/j.cstres.2025.100108, PMID 40769273.
22. Lee JH, Choi BK, Kim M, Shin HJ, Park SJ. A lucknolide derivative induces mitochondrial ROS-mediated G2/M arrest and apoptotic cell death in B16F10 mouse melanoma cells. Mar Drugs. 2024;22(12):533. doi: 10.3390/md22120533, PMID 39728108.
23. Yang W, Fan S, Ramallo-Guevara C, Kratochwil M, Thilmany S, Sugawa MD, *et al.* Persistent oxidation of mitochondrial and transmembrane proteins in rat cerebrum and heart regardless of age or nutrition. Int J Mol Sci. 2025;26(22):11155. doi: 10.3390/ijms262211155, PMID 41303639.
24. Peng Z, Gillissen B, Richter A, Sinnberg T, Schlaak MS, Eberle J. Enhanced apoptosis and loss of cell viability in melanoma cells by combined inhibition of ERK and Mcl-1 is related to loss of mitochondrial membrane potential, caspase activation and upregulation of proapoptotic Bcl-2 proteins. Int J Mol Sci. 2023;24(5):4961. doi: 10.3390/ijms24054961, PMID 36902392.
25. Lim ML, Minamikawa T, Nagley P. The protonophore CCCP induces mitochondrial permeability transition without cytochrome c release in human osteosarcoma cells. FEBS Lett. 2001;503(1):69-74. doi: 10.1016/S0014-5793(01)02693-X, PMID 11513857.
26. Vejselova Sezer C. Escin induces cell death in human skin melanoma cells through apoptotic mechanisms. Toxicol Res (Camb). 2024;13(4):tfae124. doi: 10.1093/toxres/tfae124, PMID 39108844.
27. Shao L, González-Cardenete MA, Prieto-Garcia JM. *In vitro* cytotoxic effects of ferruginol analogues in Sk-MEL28 human melanoma cells. Int J Mol Sci. 2023;24(22):16322. doi: 10.3390/ijms242216322, PMID 38003511.

28. Putri GF, Nurfatihah Z Z. Bax/Bcl-2 ratio as the golden marker of apoptosis: molecular mechanisms and regulatory pathways. CBS Int Journal. 2025;4(10):309-17. doi: 10.59278/cbs.v4i10.65.

29. Wolf P, Schoeniger A, Edlich F. Pro-apoptotic complexes of BAX and BAK on the outer mitochondrial membrane. Biochim Biophys Acta Mol Cell Res. 2022;1869(10):119317. doi: 10.1016/j.bbamcr.2022.119317, PMID 35752202.

30. Zhang Y, Bejaoui M, Linh TN, Arimura T, Isoda H. A novel amphiphilic squalene-based compound with open-chain polyethers reduces malignant melanoma metastasis *in vitro* and *in vivo*. Cell Commun Signal. 2024;22(1):437. doi: 10.1186/s12964-024-01813-5, PMID 39261954.

31. Khonsap R, Meksangsee P, Kiatwuthinon P, T-Thienprasert NP, Swainson NM, Phonphoem W *et al.* Preventive effects of *Dendrobium* hybrid extract on free radical activity and melanoma cell proliferation by inducing apoptotic gene expression. Biomed Rep. 2025;24(2):21. doi: 10.3892/br.2025.2094, PMID 41384132.

Cite this article: Hobani YH. Evaluation of the Anticancer Activity of Conessine against Human Melanoma (SK-MEL-28) Cells via Mitochondrial-Mediated Apoptotic Pathway. Indian J of Pharmaceutical Education and Research. 2026;60(4s):s1657-s1668.